New transparent electronic conductor, MgIn$_2$O$_4$ spinel

S. E. DALI, M. JAYACHANDRAN, M. J. CHOCKALINGAM
Electrochemical Materials Science Division, Central Electrochemical Research Institute, Karaikudi 630 006, Tamilnadu, India
E-mail: cecrik@cscecri.ren.nic.in

Wide band gap *n*-type oxide materials, such as Sn-doped In$_2$O$_3$, Sb-doped SnO$_2$ and Al-doped ZnO are technologically important materials and are widely used as a transparent electrode in liquid crystal display (LCD) and solar cells and are also used in heat reflector glass [1]. They often have limited applications due to their chemical instability, lack of corrosion resistivity and poor adhesion under various environments. This is due to their intrinsic properties and the methods used for preparation. Recently, excellent optical properties and chemical stability have been attained with new transparent conductive materials, such as Zn$_2$SnO$_4$, yttrium doped CdSb$_2$O$_6$, CdGa$_2$O$_4$, MgIn$_2$O$_4$ and ZnGaO$_4$ [2–4]. The resistivities obtained for these transparent conducting oxide films were 10^{-2} to 10^{-4} ohm-cm.

Chase and his co-workers [5] studied the effect of the addition of MgO up to 3.5% on the crystal growth defects and optical absorption of flux grown In$_2$O$_3$ crystal. The optical properties of such crystals resemble those of stoichiometric In$_2$O$_3$ and hence Mg is believed to compensate oxygen deficiencies within the crystal. In other words, when adding a small amount of Mg to In$_2$O$_3$, all the Mg atoms may enter substitutionally in the cation sublattice leading to a drop in the mobility. This can be avoided or reduced, if in the crystalline lattice, the doping site and conduction path of carrier electrons are separated spatially by selecting the crystal structure having two different cation sites.

In this context, mixed oxides with spinel structure are appropriate candidate materials amongst the wide band gap conductors. Further, the attractive feature of the spinel structure lies in the fact that the crystallographically equivalent planes in the lattice are occupied by cations of different valencies, between which electronic transitions may take place with negligible energy change. Magnesium indate (MgIn$_2$O$_4$) is one of the transparent electronic conductive materials which has spinel structure [6]. The conductivity has been found to be due to the electrons induced from the oxygen vacancies [7]. The distribution of cations, Mg^{2+} and In^{3+} in the tetrahedral and octahedral sites has been confirmed by Rietveld analysis approximately to be that of the inverse spinel structure, that is, in the unit cell, the two tetrahedral sites are occupied by In^{3+} and four octahedral sites are randomly occupied by Mg^{2+} and In^{3+} [6]. Kawazoe *et al.* [8] say that it was expected that magnesium indate has normal spinel structure. Two indium atoms occupy the octahedral sites and magnesium atoms occupy the tetrahedral sites so that the rutile chain

is composed of InO$_6$ octahedra. In the present case of MgIn$_2$O$_4$, normal or inverse spinel, has non occupied tetrahedral and octahedral cation sites and a well extended conduction band. As discussed earlier, the rutile chain, comprising InO$_6$ octahedra similar to SnO$_2$, has no intervening oxygen between the two neighboring M cations. Because of the covalency in M–O bonds, there is a large dispersion of the conduction band and the host material has got an extended conduction band.

In this paper, synthesis of magnesium indate by solid state reaction through nitrate and oxalate precursor routes is reported for the first time. Structural electrical and optical properties of the magnesium indate prepared are also reported here.

Polycrystalline samples of magnesium indate were synthesised by solid state reaction from two different precursors. One precursor named as sample (A), was prepared by taking the appropriate molar ratio of AR grade fine powders of MgCO$_3$ and In$_2$O$_3$ which were digested in dilute nitric acid. Another precursor, sample (B) was prepared by digesting the same stoichiometric mixture of MgCO$_3$ and In$_2$O$_3$ in 1 M of oxalic acid. The solutions of sample (A) and (B) were heated at 100 °C to get a dry mass. The mixtures thus obtained were separately well ground in an agate mortar using an acetone medium for homogeneity. The resulting powders were calcined at 900 °C for 24 h and made into pellets of 12 mm diameter and 2 mm thickness using Peeco hydraulic press at a pressure of 2 ton cm^{-2}. Then the pellets were sintered at higher temperatures ranging from 1000 to 1300 °C for a duration of 24–60 h. The atmosphere used for firing was air in all cases.

The crystalline phase formed was identified with an X-ray diffractometer (JEOL JDX-803a) using CuK_α radiation in the 2θ range 10–85°. The instrument was operated at 40 kV and 20 mA. Powder X-ray diffraction patterns of the sample (A) and (B) heated at different temperatures ranging from 900–1300 °C are shown in Figs 1 and 2. At 900 °C, all the peaks correspond to MgO and In$_2$O$_3$. The formation of MgIn$_2$O$_4$ was initiated at 1000 °C. As the temperature increased, the percentage of MgIn$_2$O$_4$ formation also increased in both samples. Monophase formation of MgIn$_2$O$_4$ was formed in sample (B) when it was heated at 1300 °C for 60 h and in sample (A), 13.65% of In$_2$O$_3$ was present in the final product. The percentage of phase formation at different temperatures is tabulated in Table I and is shown in Fig. 3. The phase formation is estimated from
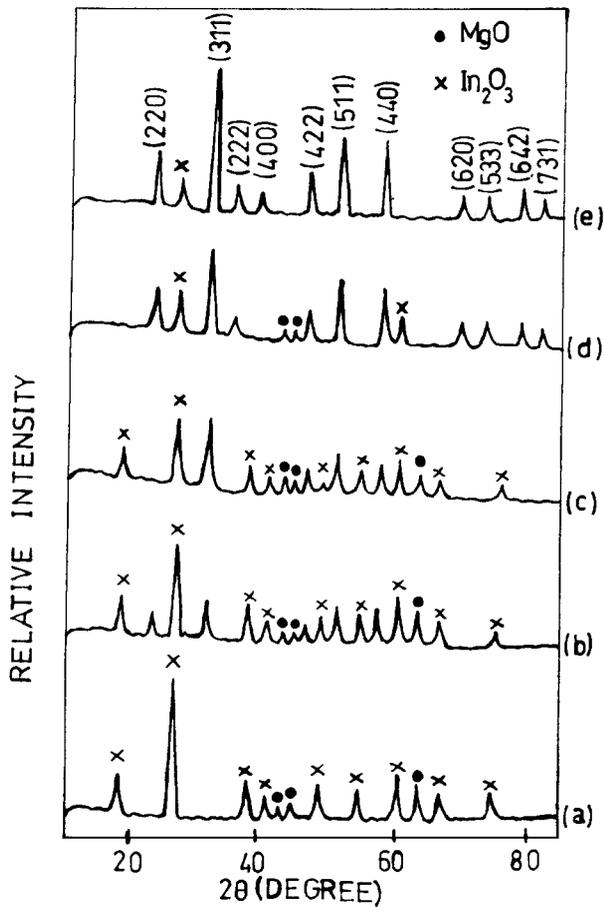
Figure 1 Powder X-ray diffraction patterns of sample (A) heated at (a) 900 °C, (b) 1000 °C, (c) 1100 °C for 24 h, (d) 1200 °C for 48 h and (e) 1300 °C for 60 h.
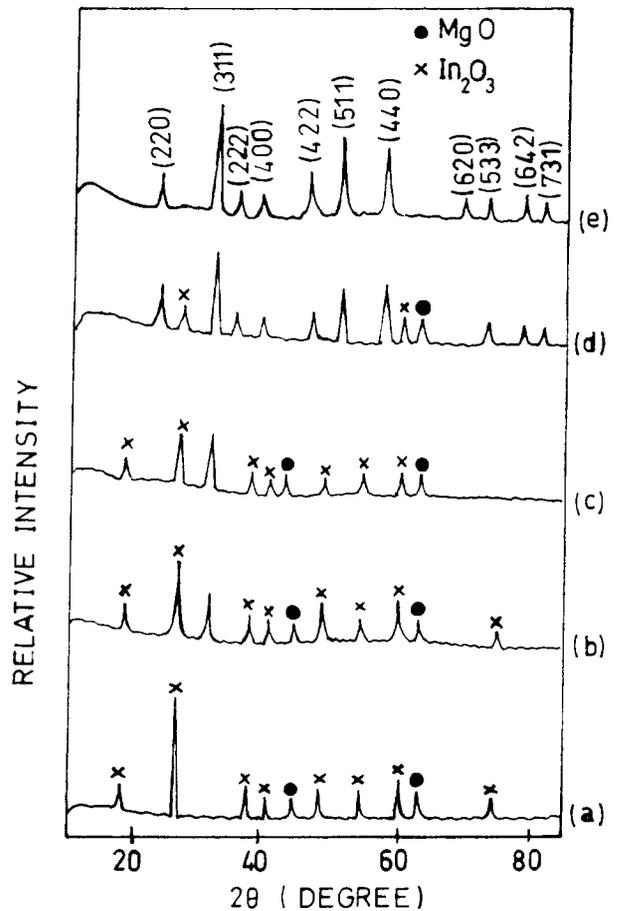

Figure 2 Powder X-ray diffraction patterns of sample (B) heated at (a) 900 °C, (b) 1000 °C, (c) 1100 °C for 24 h, (d) 1200 °C for 48 h and (e) 1300 °C for 60 h.

the relation [9],

$$\% \text{ of MgIn}_2\text{O}_4 = \frac{I_{\text{MIO}}}{I_{\text{MIO}} + I_{\text{MO}} + I_{\text{IO}}} \times 100$$

where I_{MIO} is the maximum intensity of MgIn$_2$O$_4$ peak; I_{MO}, the maximum intensity of MgO peak; and I_{IO}, the maximum intensity of In$_2$O$_3$ peak.

The d.c. electrical resistivity of the pellets of sample (A) and (B) heated at 1300 °C for different durations was measured by a 2 probe technique and is tabulated in Table II. Log ρ versus synthesis time at 1300 °C for both samples is shown in Fig. 4. The pellet of sample (B) showed lower resistivity than sample (A). Heat-

ing of the pellets for a longer duration decreased the resistivity of the pellet in both cases. At 1300 °C for 60 h heating, the resistivity values of sample (A) and (B) were 5.01×10^1 ohm-cm and 7.07×10^0 ohm-cm

TABLE I Percentage of phase formation of samples (A) and (B) at different temperatures

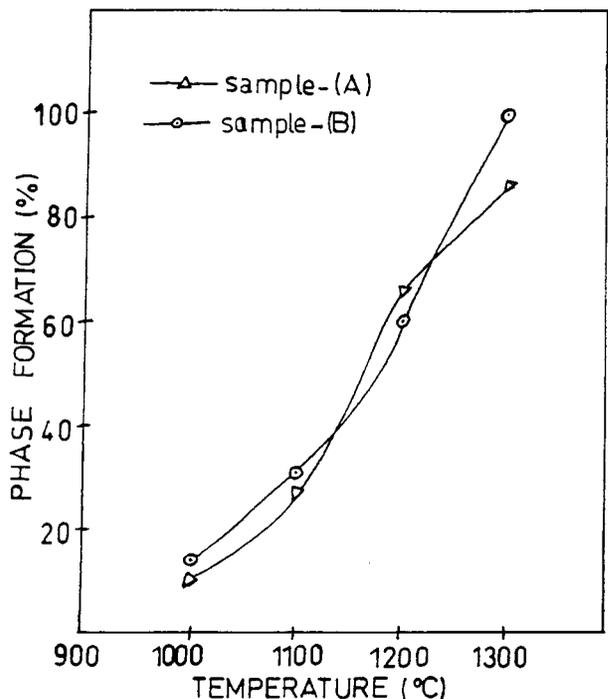| Sample	Temperature (°C)	MgO (%)	In$_2$O$_3$ (%)	MgIn$_2$O$_4$ (%)
(A)	900	14.29	85.71	—
	1000	12.65	75.96	11.39
	1100	9.47	62.85	27.68
	1200	7.36	25.77	66.87
	1300	—	13.65	86.35
(B)	900	13.36	86.64	—
	1000	10.08	75.72	14.20
	1100	8.27	60.46	31.27
	1200	4.14	35.12	60.74
	1300	—	—	100.00

Figure 3 Percentage of MgIn$_2$O$_4$ phase formation at different temperatures for samples (A) and (B).

TABLE II Resistivity of $MgIn_2O_4$ pellets sintered at 1300 °C for different durations

Synthesis time (h)	Sample (A)		Sample (B)	
	Resistivity, ρ (Ohm-cm)	Log ρ	Resistivity, ρ (Ohm-cm)	Log ρ
0	5.62×10^6	6.75	2.51×10^6	6.4
12	1.78×10^5	5.25	5.62×10^4	4.75
24	2.04×10^4	4.31	3.72×10^3	3.57
36	3.98×10^3	3.6	5.62×10^2	2.75
48	3.16×10^2	2.5	5.01×10^1	1.7
60	5.01×10^1	1.7	7.07×10^0	0.85

Figure 5 Diffuse reflectance spectra of (a) sample (A), (b) sample (B) and (c) In_2O_3.

respectively. The resistivity value of sample (B) was found to decrease less than that of sample (A).

The diffuse reflectance spectra of samples (A) and (B) were taken using a Hitachi U3400 UV-Vis-NIR spectrophotometer in the wavelength range 350–600 nm and are shown in Fig. 5.

The spectrum of the standard In_2O_3 powder was also taken for comparison. An Al_2O_3 disc was used as reference. From the diffuse reflectance spectra, a reduction of reflectance was observed for samples (A) and (B) above 450 nm when compared with In_2O_3. The fundamental absorption edge of $MgIn_2O_4$ appears near 382 nm and is at a shorter wavelength than that of In_2O_3. This observation shows that the band gap of $MgIn_2O_4$ ($\sim$3.3 eV) is much higher than that of the In_2O_3.

In conclusion, $MgIn_2O_4$ has been prepared by solid state reaction through nitrate and oxalate precursor routes. Out of these two routes, the oxalate precursor route [sample (B)] gives monophase $MgIn_2O_4$ at
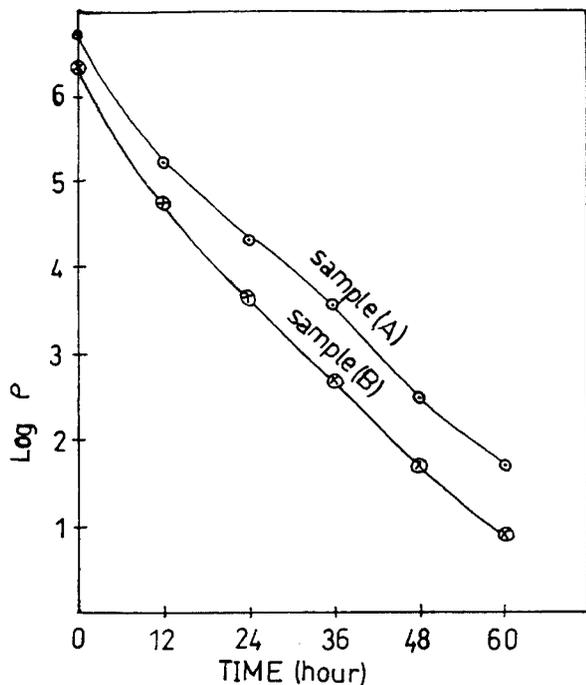
1300 °C after 60 h heating. In the nitrate precursor route [sample (A)], about 13.65% of In_2O_3 was present in the final product. This shows that oxalic acid precursor route gives better phase formation than the nitrate precursor route. The structure was observed to be cubic spinel. The d.c. electrical resistivity of the pellets of samples (A) and (B) were 5.01×10^1 ohm-cm and 7.07×10^0 ohm-cm respectively. From the observation, the resistivity value of sample (B) is decreased about one order compared to sample (A). This shows that magnesium indate prepared by oxalate precursor route has better conductivity than the samples prepared by nitrate precursor route. By the measurements of diffuse reflectance spectra, the optical band gap of $MgIn_2O_4$ ($\sim$3.3 eV) was found to be wider than that of In_2O_3. Based on all the above results, we conclude that magnesium indate prepared by oxalate precursor route has better phase formation and conductivity than the sample prepared by nitrate precursor route.

Figure 4 Log ρ versus time graph of sample (A) and (B) pellets sintered at 1300 °C for different durations.

References

1. K. L. CHOPRA, S. MAJOR and D. K. PANDYA, *Thin Solid Films* **102** (1983) 1.
2. T. MINAMI, S. TAKATA, T. KAKUMU and H. SONOHARA, *ibid.* **270** (1995) 22.
3. T. OMATA, N. UEDA, N. HIKUMA, K. UEDA, H. MIZOGUCHI, T. HASHIMOTO and H. KAWAZOE, *Appl. Phys. Lett.* **62** (1993) 499.
4. T. OMATA, N. UEDA and K. UEDA, *ibid.* **64** (1994) 1077.
5. A. B. CHASE and H. H. TIPPINS, *J. Appl. Phys.* **38** (1967) 2469.
6. N. UEDA, T. OMATA, N. HIKUMA and H. KAWAZOE, *Appl. Phys. Lett.* **61** (1992) 1954.
7. H. UN'NO, N. HIKUMA, T. OMATA, N. UEDA, T. HASHIMOTO and H. KAWAZOE, *Jpn. J. Appl. Phys.* **32** (1993) L1260.
8. H. KAWAZOE, N. UEDA, H. UN'NO, T. OMATA, H. HOSONO and H. TANOUE, *J. Appl. Phys.* **76** (1994) 7935.
9. MING-CHRONG JIANG, TAN-JUE HONG and TAI-BOR WU, *Jpn. J. Appl. Phys.* **33** (1994) 6301.